

A STUDY ON SHEAR CAPACITY OF RC BEAM BASED ON FRACTURE MECHANICS

A. Masuda, S. Matsuoka, and Y. Takeda,
Institute of Technology, Tekken Corporation, Narita, Japan
T. Watanabe,
Hokubu Consultant Corporation, Sapporo, Japan

Abstract

The shear failure behavior of reinforced concrete was analyzed using the finite element method with the concepts of fracture mechanics. The analytical model developed for this purpose considers tensile stress attenuation at cracks, localization of cracks, and shear force transmitted through cracks in order to ensure that shear failure behaviors of reinforced concrete components can be traced. The shear force transmitted through cracks, is assumed in this model to be a force decreasing along with crack opening. In addition, to verify that this analysis is appropriate, the size dependency of calculated shear strength is compared with the experimental results.

Key words : fracture mechanics, shear failure, RC beam

1 Introduction

Since concrete fracture is dominated by cracking and its propagation, the fracture mechanics describing the mechanical behavior related to crack initiation and propagation is effective for structural analysis of concrete. Therefore, the mechanical properties of cracking have been

investigated by many researchers.

When the sectional force of concrete members is determined by shear fracture, cracks occur in mixed mode (Mode I plus Mode II). The authors proposed a mode for simulating fractures in mixed mode, on the basis of the smeared crack modelling technique. This technique can simulate cracks at any location, unlike the discrete crack model for which the cracking position should be determined in advance.

By resorting to the smeared crack model, computations on RC beams were conducted to demonstrate that this analytical technique is capable of assessing the size dependency of shear strength.

2 Summary of analytical techniques

2.1 Tensile fracture characteristics of concrete

Hordijk(1991) proposed, on the basis of tensile test results of concrete, approximation by Eq. (1) of the tension softening curve.

$$\frac{\sigma_t}{f_t} = \left\{ 1 + \left[C_1 \frac{w}{w_c} \right]^3 \right\} \exp \left[- C_2 \frac{w}{w_c} \right] - \frac{w}{w_c} \left[1 + C_1^3 \right] \exp(- C_2) \quad (1)$$

where $C_1=3$, $C_2=6.93$, w represents crack opening width, w_c is limit opening width ($=160 \mu m$), f_t is tensile strength of concrete, σ_t is tensile stress with crack opening width w . Planas et al.(1995) reported, on the basis of experiments and analysis, an effective approximation of the maximum load of concrete. He used a straight-line model, whose gradient is that of the tension softening curve at the point immediately after crack initiation. Accordingly, as shown in Fig. 1 the tensile fracture characteristic of concrete is expressed in this paper by a straight line with a gradient of the tangent to the curve at the point immediately after crack initiation of Eq. (1).

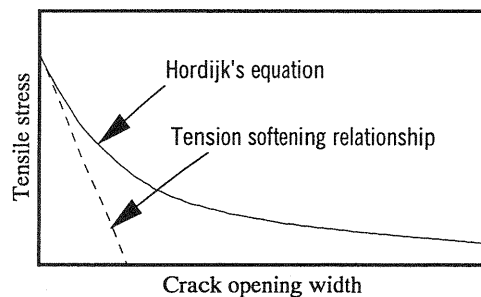


Fig. 1. Tension softening relationship

2.2 Judgment for localization of cracks

For studying the crack localization in brittle materials such as concrete, it is necessary to judge whether the tensile characteristic of the cracked elements is on the unloading path or on the tension softening curve. In the present study, we made our calculations assuming the cracked elements are on the tension softening curve. Then, at the next increment, we assumed that the same elements are on the unloading path in the direction of the origin. In this incremental computation, when the tensile characteristic of the cracked elements is outside the tension softening curve, computation is redone, considering that the tensile characteristic should be on the tension softening curve instead of on the unloading path. By such repetitive computations, the crack was localized.

2.3 Shear stiffness of the cracked elements

The shear retention factor is introduced here, which is determined by Eq. (2). It is a dimensionless expression of the shear stiffness of the cracked elements in terms of the shear stiffness before cracking.

$$\beta = \exp(-\alpha \cdot w) \quad (2)$$

where β is the shear retention factor, α is the decrease rate of shear retention factor, w is the crack opening width. The decrease rate of the shear retention factor was determined such that the tangent gradient of the shear retention factor just after crack initiation is equal to the gradient of tension softening curve as shown in Fig. 2.

For the compressive stress-strain curve, a quadratic expression was selected. The yield theory we used is based on the Drucker-Prager's conical expression. Supposing the compressive stress-strain relationship be a curve given by a uni-axial test, the constants of the yield equation were determined.

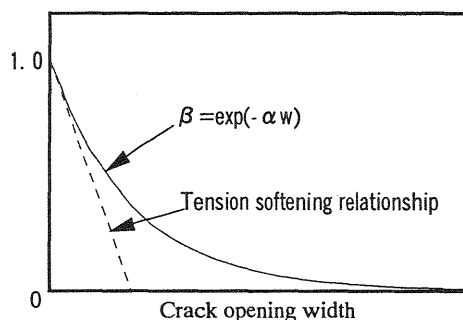


Fig. 2. Definition of shear retention factor

3 Bonding between reinforcement and concrete

To make the proposed model applicable also to RC structures, it is necessary to study the bonding between concrete and reinforcing bars. Accordingly, analysis was conducted on the Shima et al.'s tensile tests(1987) of the reinforcement embedded in concrete, to verify that the model can be applied.

Table 1. Physical properties of the test specimen material

Pattern	Concrete compressive strength (MPa)	Tension reinforcement ratio (%)	Reinforcement yield strength (MPa)	Reinforcement elastic modulus (GPa)
A	25	0.6	610	190
B			350	

Fig. 3 is the schematic diagram of the test specimen. Table 1 shows the properties of the test specimen materials. The analysis was done on two types of tests, which differed in reinforcement material only. The reinforcing bars are modeled by truss elements, which do not bear the force of bending. Since the analysis is aimed at following the RC beam shear fracture resulting from diagonal cracking, a perfect elasto-plastic model is created for representing the reinforcement. The tensile strength was estimated from the compressive strength using Eq. (3) proposed by Koenig et al. (1993)

$$f_t = 2.12 \times \ln \left(1 + \frac{f_c}{10} \right) \quad (3)$$

where f_t is the tensile strength and f_c is the compressive strength. Referring to this tensile strength and Fig. 1, the tension-softening curve was assumed to be given by Eq. (4).

$$f_t = -133 w + 2.66 \quad (4)$$

The shear retention factor given by Eq. (5) was applied, which was obtained from the tension-softening curve.

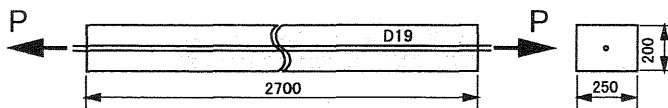


Fig. 3. Diagram of reinforcement pull-out test

$$\beta = \exp(-50w) \quad (5)$$

The graphs in Fig. 4 are load-displacement curves constructed from experimental and numerical results. The loads are tensions on the reinforcement. The displacements are average strains obtained by dividing the reinforcing bar displacement by the specimen length. The experimental results show that, in the range of the average strain up to around 0.1%, the concrete will fracture, resulting in reduced bonding with the reinforcement. When the strain exceeds 0.2%, no bonding remains, and the loads are borne by the reinforcement alone. We can assume, therefore, the maximum load depends upon the reinforcing bar material. When the reinforcing bars yield, the slope of the load increase becomes extremely gentle.

The numerical results are summarized as follows. There is a region for both patterns, where the load slightly fluctuates at 0.1MN, while the average strain alone increases. This region corresponds to the phase in which cracks appear normal to the reinforcement successively from both ends of the specimen toward the center at certain intervals. Finally, cracks are distributed with almost uniform spacing in the whole of the specimen, and the load stops fluctuating. We can conclude that such regions as that above depend on the nature of the concrete. The fluctuations analytically observed agree well with the experimental results. After this phase, the load increases due to the rigidity of the reinforcing bars, and ultimately, the bars yield, resulting in utterly no load increase. This behavior was obtained because of the analytical assumption of the stress-strain relationship of reinforcing bars being perfect elasto-plastic. Nevertheless, we can conclude that there is a good agreement between analytical and experimental results.

Fig. 5 shows the distribution of stress in reinforcement immediately after yielding. The experimental results show, for both patterns, an

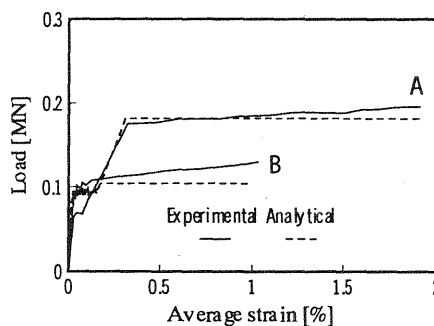


Fig. 4. Load-strain curve

undulating distribution of stresses around the yield stress. That is to say, the stress reaches the yield point at multiple locations, causing bonding between reinforcement and concrete to be broken, and consequently resulting in the near-yield state along the whole length of the bar. The analytical stress distributions have smaller undulating cycles, which are nearly one half of the specimen sectional height. Almost all the stress magnitudes are below the yield point. However, some do reach the yield point, which may be why the load does not increase. This state corresponds to cracking in concrete, where cracks occur at intervals due to bending in the RC beams.

As discussed above, the model proposed here is capable of analyzing the crack initiation and propagation in concrete structures.

4 Size effect of shear strength

Iguero et al.(1984) reported a study on the size effect of shear strength, and on the basis of bending tests with RC beam specimens of 10 cm to 300 cm in effective sectional height, which were not provided with shear reinforcement. Fig. 6 shows schematically the bending test. Tables 2 and

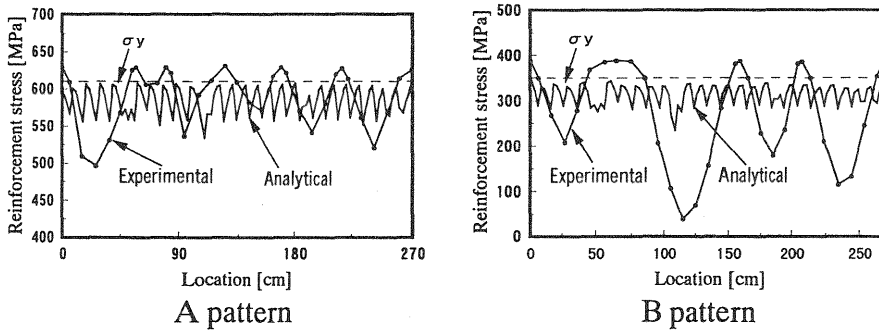


Fig. 5. Stress distribution in reinforcement

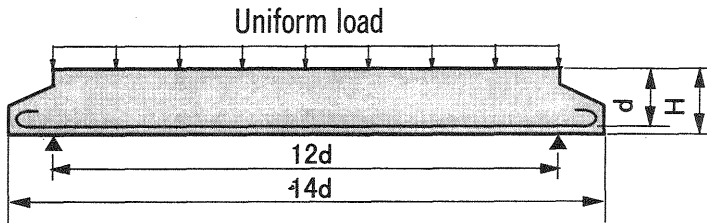


Fig. 6. Diagram of beam bending test

3 list the specification and properties, such as sectional dimensions. The proposed analytical model was applied to these experiments. Since the concrete strength varies slightly with specimen as shown in Table 3, the analysis used the value of 23.5 MPa, which is the required average strength of mixture. The shear retention factor determined with Eq. (5) was used.

Table 2. Test specimen dimensions

Effective height d(cm)	Loading span 12d(cm)	Loading span ratio	Total length 14d(cm)	Total height H(cm)	Total Width b(cm)
10	120	12	140	12	15.8
20	240		280	22	15.8
60	720		840	65.5	30
100	1200		1400	120	50
200	2400		2800	210	100
300	3600		4200	314	150

Table 3. Test specimen properties

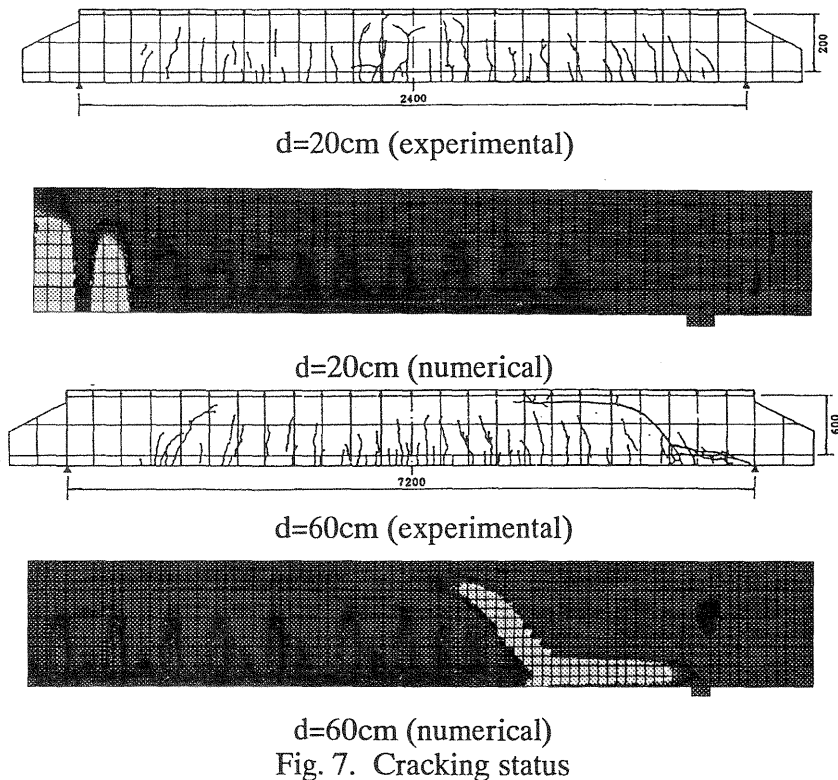
Effective height d(cm)	Concrete			Reinforcement	
	Coarse Aggregate Size (mm)	Compressive strength (MPa)	Tensile Strength (MPa)	Reinforcement ratio in the axial direction (%)	Yield Strength (MPa)
10	10	20.6	1.85	0.4	440
20		19.7	1.87		
60		21.1	1.81		
100		27.2	2.05		
100	25	21.9	2.23		370
200		28.5	2.73		
300		24.3	2.19	360	

According to Iguro et al., with specimens of 20 cm or less in effective sectional height, the main reinforcement yields. Therefore, the strength is determined by the bending fracture, whereas, with specimens of 60 cm or more in sectional height, shear fracture was observed, where the strength is determined by the diagonal crack initiation and propagation. For example, no diagonal cracking is found in the specimen of 20 cm in

effective sectional height shown in Fig. 7. In contrast, diagonal cracking is observed in the specimen of 60 cm in effective sectional height. Such cracking pattern demonstrates that a shear fracture takes place.

The diagrams in Fig. 7 are the cracking patterns numerically created for the cases of 20 cm and 60 cm in effective sectional height. In the case of 20 cm, there is no diagonal crack in the analytical result too, whereas, in the case of 60 cm, diagonal cracking occurs. In the analysis, since the diagonal crack reached the compressive side edge, the computation was finished. Therefore, in the analysis too, with the effective sectional height of 60 cm, the strength is determined by the diagonal crack initiation and propagation, that is to say, shear fracture occurs. With effective sectional heights more than 60 cm, the strength is governed by the diagonal cracking.

The relationship between main reinforcement strain and load is shown in Fig. 8. In the case of 20 cm effective sectional height, the analytical results show that the main reinforcement strain will certainly reach the yield point (0.0018), whereas in the experiment, the measurement became impossible when the main reinforcement strain exceeds the yield point. Thus, both numerically and experimentally, the strength is governed by



d=60cm (numerical)
Fig. 7. Cracking status

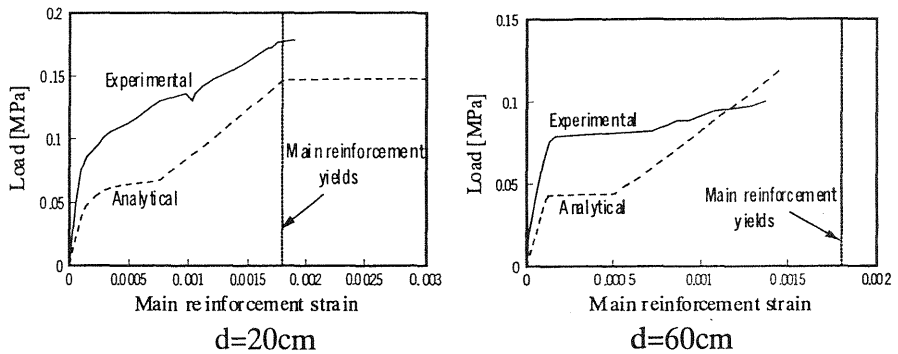


Fig. 8. Relationship between load and strain of main reinforcement

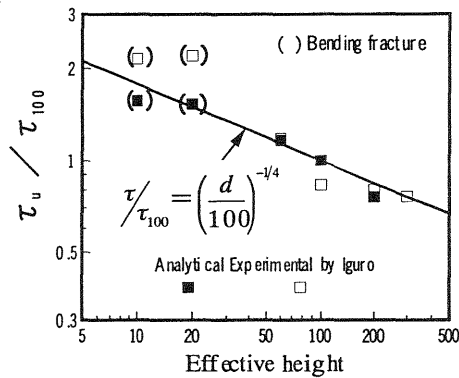


Fig. 9. Size effect of shear strength

bending fracture. In the case of 60 cm effective sectional height, the ultimate strain of the main reinforcement is below the yield both numerically and experimentally. Hence, the strength is determined by the shear fracture.

Fig. 9 shows the relationship between shear strength of concrete and effective sectional height. The solid line in the figure represents the size effect of shear strength of concrete proposed by Iguro et al. on the basis of the experimental results. The analytical results agree well with the experimentally determined size effect on shear strength.

This verifies the effectiveness of the proposed model for computing the shear strength size effect of RC beams.

5 Conclusions

The effectiveness of the proposed model when used for RC structures was demonstrated, for analyzing structures undergoing shear fracture, the

ultimate strength of which is governed by diagonal crack propagation. The conclusions of this study show that:

- By incorporating the reinforcement expressed by truss elements, which have no bending stiffness, into the proposed model, we are able to determine the fracture behavior of RC structures. In this analysis, the decrease in bonding between reinforcement and concrete is expressed by the fracture in concrete near the reinforcement, which does not require any special model.
- The proposed model was applied to the previous experimental results on RC components. Through comparison of numerical and experimental results, we can confirm that the computed cracking patterns and ultimate strength are reasonable values. Furthermore, good agreement with experimental outputs has been found for determining the bending and shear fracture mode, and the size effect of shear strength.

References

- Hordijk, P.A. (1991) Local Approach to Fatigue of Concrete, Doctoral Thesis, **Delft University of Technology**.
- Iguro, M., Shioya, T., Nojiri, Y. and Akiyama, H. (1984) Experimental Studies on The Shear Strength of Large Reinforced Concrete Beams under Uniformly Distributed Load, in **J. Materials, Conc. Struct., Pavements, JSCE**, NO.348/V -1 (report), 175-184.
- Koenig, G., Grimm, R. and Rimmel, G. (1993) Shear Behavior of Longitudinally Reinforced Concrete Members of HSC, in **JCI International Workshop on Size Effect in Concrete Structures**, 63-74.
- Matsuoka, S., Masuda, A., Takeda, Y. and Doi, S. (1997) Analytical model for concrete structures influenced by crack initiation and propagation, to be submitted to **Proceedings of JSCE**.
- Planas, J., Guinea, G.V. and Elices, M. (1995) Rupture Modulus and Fracture Properties of Concrete, in **Fracture Mechanics of Concrete Structures** (eds. F.H. Wittmann), FRAMCOS-2, 95-110.
- Shima, H., Chou, L. and Okamura, H. (1987) Micro and Macro Models for Bond in Reinforced Concrete, in **Journal of The Faculty of Engineering**, The University of Tokyo (B), Vol.XXXIX, No.2, 133-194.